Journal of the Serbian Society for Computational Mechanics / Vol. 15 / No. 1, 2021 / pp 51-64
(10.24874/jsscm.2021.15.01.04)

SORET AND VARIABLE THERMAL CONDUCTIVITY EFFECTS ON HYDRO-MAGNETIC RADIATING FLUID PAST A VERTICAL PLATE WITH POROUS MEDIUM

M. Santha Raju [1*], G.S.S. Raju[2]

[1] Department of Mathematics, JNT University Anantapur, Ananthapuramu, Andhra Pradesh, India
e-mail: santharajusrkgac@gmail.com
[2] Department of Mathematics, JNTUA College of Engineering, Pulivendula, Andhra Pradesh, India
e-mail: rajugss@yahoo.com
** corresponding author*

Abstract

Thermal diffusion and variable thermal conductivity effects on unsteady magnetohydrodynamic (MHD), heat and mass transfer flow past an infinite vertical porous plate have been investigated and analyzed numerically. The resultant flow governing equations are resolved numerically by the finite-difference scheme of the Crank-Nicolson type implicit method. The non-dimensional velocity, fluid temperature, and species concentration distributions are conferred through graphs for different fluid parameters involved such as Joule-heating parameter, suction parameter, chemical reaction parameter, radiation parameter, etc. The coefficient of skin friction, Nusselt number and Sherwood number were tabulated. The concentration of the fluid rises with an increase in Soret number, whereas the Sherwood number reduces due to its increase.

Keywords: Magnetohydrodynamic, heat and mass transfer, Soret effect, variable thermal conductivity, implicit finite difference scheme.

1. Introduction

The heat and mass exchange measure happen regularly in nature. It occurs due to the difference in temperature or difference in concentration, or both, in different geophysical cases. It has been considered by theoretical, experimental studies having their wide applications, such as heat exchangers for the packed bed, heat insulation, energy-storage units, catalytic reactors, geothermal systems, drying technology, and nuclear waste repository. The convective flow and heat transfer of fluid in porous media in the presence of the magneto-hydrodynamic (MHD) field has special technical significance. Hence, many researchers are attracted due to numerous applications in various branches of engineering. Jha (1994) studied the effect of the heat source and magnetic effect on the hydro-magnetic free convective flow of a non-conducting vertical porous plate. Chamkha (2004) discussed the influence of heat absorption and buoyancy effect on hydro-magnetic fluid flow past a permeable moving plate with the magnetic field. Mahamadien (2012) investigated the thermal dispersion influence on MHD convective laminar flow. In his study, the thermal dispersion parameter was observed proportional to dimensionless velocity and dimensionless temperature. Ahmed and Kalita (2013) evaluated the variation of radiation and chemical reaction effect on hydro-magnetic flow over an oscillating plate numerically and analytically. Uwanta and Sani (2014) investigated the effects of variable thermal conductivity, chemical reaction, and heat source on MHD flow past a vertical plate. Javaherdeh et al. (2015) investigated free convection heat and mass transfer for MHD flow past a vertical porous plate with the transverse magnetic field by numerical method. Praveena et al. (2017) investigated analytical explanations to free convective, electrically conducting, viscous flow of a micropolar fluid embedded in a porous plate with chemical reaction and heat generation. Sarma and Pandit (2016) studied the exact solution on Soret, rotation and Hall effects on hydro-magnetic flow fluid on a vertical porous plate. Krishna and Reddy (2018) presented the influences of the heat source and chemical reaction on magneto-hydrodynamic flow through a porous medium past a moving plate. Reddy et al. (2016), Murthy and Kumar (2018) and Idowu and Falodun (2019) studied the influence of diffusion thermo (Dufour) and thermal diffusion (Soret) on different fluids. Investigations of Soret, Hall and Joule's effects on the hydro-magnetic flow of a viscous fluid past a vertical plate through a porous medium were investigated by Krishna et al. (2019). Ahmed et al. (2013) investigated the exact solution for the influence of thermal diffusion on MHD free convective flow past an oscillating vertical plate with a porous medium. In their investigation, identified fluid concentration rose, and velocity accelerated due to the Soret effect. Reddy PC et al. (2018) investigated the exact solution of the heat source effect on MHD convective radiating flow fluid past a vertical plate with a porous medium. Reddy KS et al. (2018) studied the effect of thermal diffusion on Newtonian MHD fluid past a vertical plate with a porous medium. In the paper, they concluded that the Soret effect enhances the concentration of the fluid and falls down the skin friction coefficient.

The purpose of the current examination is to extend the work of Uwanta and Sani (2014) by adding the thermal diffusion (Soret) effect to the mass concentration equation so that systems of equations are coupled. The second-order partial differential equations with boundary conditions are resolved by an implicit finite-difference scheme. The impact of different parameters on non-dimensional parameters - velocity, temperature, and species concentration of flow, was conferred through figures. The skin friction coefficient, numbers of Nusselt and Sherwood were observed through tables.

2. Mathematical formulation

An incompressible, unsteady, electrically-conducting, radiating, heat-absorbing, one-dimensional fluid flow is considered past an infinite porous vertical plate. $\bar{x}$ - axis is taken along the vertical plate towards the upward direction, and $\bar{y}$ - axis is normal to it. The magnetic fluid B_0 is presumed to be acting in the perpendicular direction of the fluid flow. The presence of the Soret effect is also considered. Since the length of the plate is infinite, the basic fluid parameters depend on the time $\bar{t}$ and space coordinate $\bar{y}$ only. At the time $\bar{t} \leq 0$, both fluid and plate are maintained at the same temperature $\bar{T}_\infty$ and concentration $\bar{C}_\infty$ at all points, respectively. For time $\bar{t} > 0$, the plate is fixed, whereas the fluid temperature and species concentration at the plate are upraised to $\bar{T}_w$ and $\bar{C}_w$ respectively. The flow geometry and its coordinate system are presented in Fig. 1.

Based on the above suppositions and the Boussinesq's approximation, the resultant fluid flow equations, i.e., continuity, momentum, mass-energy, and concentration (Sharma et al. 2005, Ahmed et al. 2013), respectively are given below:

$$\frac{\partial \bar{v}}{\partial \bar{y}} = 0 \tag{1}$$

$$\frac{\partial \bar{u}}{\partial \bar{t}} + \bar{v}\frac{\partial \bar{u}}{\partial \bar{y}} = \nu \frac{\partial^2 \bar{u}}{\partial \bar{y}^2} - \frac{\sigma B_0^2 \bar{u}}{\rho} - \frac{\nu \bar{u}}{\bar{K}} + g\bar{\beta}\left(\bar{C} - \bar{C}_\infty\right) + g\beta\left(\bar{T} - \bar{T}_\infty\right) - \bar{b}_1 \bar{u}^2 \tag{2}$$

$$\frac{\partial \bar{T}}{\partial \bar{t}} + \bar{v}\frac{\partial \bar{T}}{\partial \bar{y}} = \frac{1}{\rho C_p}\frac{\partial}{\partial \bar{y}}\left(K\left(\bar{T}\right)\frac{\partial \bar{T}}{\partial \bar{y}}\right) - \frac{1}{\rho C_p}\frac{\partial q_r}{\partial \bar{y}} + \frac{\nu}{C_p}\left(\frac{\partial \bar{u}}{\partial \bar{y}}\right)^2 + \bar{b}\bar{u}^2 - \frac{Q}{\rho C_p}\left(\bar{T} - \bar{T}_\infty\right) \tag{3}$$

$$\frac{\partial \bar{C}}{\partial \bar{t}} + \bar{v}\frac{\partial \bar{C}}{\partial \bar{y}} = D_M \frac{\partial^2 \bar{C}}{\partial \bar{y}^2} + D_T \frac{\partial^2 \bar{T}}{\partial \bar{y}^2} - \bar{R}\left(\bar{C} - \bar{C}_\infty\right)^n \tag{4}$$

The following initial & boundary conditions are

$$\begin{aligned} &\bar{t} \le 0,\ \bar{u}\left(\bar{y},\bar{t}\right) = 0, \bar{T}\left(\bar{y},\bar{t}\right) = \bar{T}_\infty, \bar{C}\left(\bar{y},\bar{t}\right) = \bar{C}_\infty \text{ for all } \bar{y} < 0 \\ &\bar{t} > 0,\ \bar{u}\left(\bar{y},\bar{t}\right) = 0, \bar{T}\left(\bar{y},\bar{t}\right) = \bar{T}_w, \bar{C}\left(\bar{y},\bar{t}\right) = \bar{C}_w \text{ at } \bar{y} = 0 \\ &\qquad \bar{u}\left(\bar{y},\bar{t}\right) = 0, \bar{T}\left(\bar{y},\bar{t}\right) = \bar{T}_\infty, \bar{C}\left(\bar{y},\bar{t}\right) = \bar{C}_\infty \text{ as } \bar{y} \to \infty \end{aligned} \tag{5}$$

Where $\bar{t}, Q, \bar{T}, \bar{C}, \bar{T}_\infty, \bar{C}_\infty, \bar{T}_w, \bar{C}_w, \nu, B_0, \sigma, \bar{K}, \beta, \bar{b}_1, \bar{\beta}, g, D_T, D_M, \bar{R}, C_P, q_r, \bar{b}, K\left(\bar{T}\right), \rho$ represent dimensional time, volumetric rate of heat generation, temperature of the fluid, species concentration of the fluid, free stream temperature, free stream concentration, surface temperature, surface concentration, kinematic viscosity, constant magnetic field intensity, Stefan Boltzmann constant, thermal expansion coefficient, Forchheimer parameter of the medium, concentration expansion coefficient, gravitational constant, thermal diffusivity coefficient, chemical molecular diffusivity coefficient, chemical reaction, specific heat at constant pressure, radiative heat flux, Joule-heating parameter, the variable thermal conductivity, density. $(\bar{u}, \bar{v})$ represents fluid velocity corresponding $\bar{x}$ and $\bar{y}$ directions.

The continuity Eq. (1) on integration, we get $\bar{v} = -v_0$, for any $v_0 > 0$, where v_0 is suction velocity. The radiative heat flux can be written by Rosseland approximation as

$$\frac{\partial q_r}{\partial \bar{y}} = -4\sigma\bar{a}\left(\bar{T}_\infty^4 - \bar{T}^4\right) \tag{6}$$

Now, we expand $\bar{T}^4$ into about $\bar{T}_\infty$ in series form, and we get

$$\bar{T}^4 \simeq 4\left(\bar{T} - \bar{T}_\infty\right)\bar{T}_\infty^3 + \bar{T}_\infty^4 \simeq 4\bar{T}\bar{T}_\infty^3 - 3\bar{T}_\infty^4 \tag{7}$$

The temperature-dependent variable thermal conductivity (Abel et al. 2009) is given by

$$K\left(\bar{T}\right) = \left[\delta(\bar{T} - \bar{T}_\infty) + 1\right]k_\alpha \tag{8}$$

where the k_α is the fluid thermal conductivity and δ is the constant.

3. Method of solution

The following non-dimensional variables are defined to obtain non-dimensional partial differential equations (PDE)

$$U=\frac{\bar{u}}{U_0}, y=\frac{\bar{y}U_0}{\nu}, t=\frac{\bar{t}U_0^2}{\nu}, \theta=\frac{\bar{T}-\bar{T}_\infty}{\bar{T}_w-\bar{T}_\infty}, C=\frac{\bar{C}-\bar{C}_\infty}{\bar{C}_w-\bar{C}_\infty}, \tau=\delta\left(\bar{T}-\bar{T}_\infty\right), b=\frac{\bar{b}\nu}{\bar{T}_w-\bar{T}_\infty},$$
$$Sc=\frac{\nu}{D_M}, \Pr=\frac{\nu\rho C_P}{k_\alpha}, Ec=\frac{U_0^2}{C_P\left(\bar{T}_w-\bar{T}_\infty\right)}, Gr=\frac{g\beta\nu\left(\bar{T}_w-\bar{T}_\infty\right)}{U_0^3}, Gc=\frac{g\bar{\beta}\nu\left(\bar{C}_w-\bar{C}_\infty\right)}{U_0^3},$$
$$\alpha=\frac{\nu_0}{U_0}, K=\frac{\bar{K}U_0^2}{\nu}, N=\frac{16\bar{a}\sigma\bar{T}_\infty^3\nu^2}{k_\alpha U_0^2}, M=\frac{\nu\sigma B_0^2}{\rho U_0^2}, b_1=\frac{\bar{b}_1\nu}{U_0}, S=\frac{Q\nu^2}{k_\alpha U_0^2},$$
$$S_0=\frac{D_T}{\nu}\left(\frac{\bar{T}_w-\bar{T}_\infty}{\bar{C}_w-\bar{C}_\infty}\right), Kr=\frac{\nu\bar{R}\left(\bar{C}_w-\bar{C}_\infty\right)^{n-1}}{U_0^2} \tag{9}$$

Where U_0 is the non-dimensional constant.

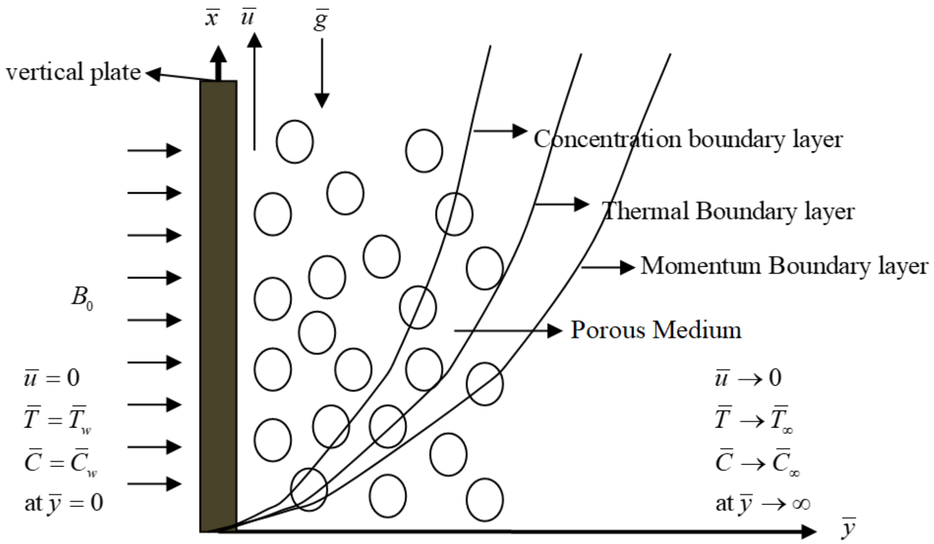

Fig. 1. Flow geometry and coordinate system.

By introducing the above dimensionless variables from equation (9), then the equations (2)-(4) are converted as follows:

$$\frac{\partial U}{\partial t}-\alpha\frac{\partial U}{\partial y}=\frac{\partial^2 U}{\partial y^2}-\left(M+\frac{1}{K}\right)U+Gr\theta+GcC-b_1U^2 \tag{10}$$

$$\frac{\partial\theta}{\partial t}-\alpha\frac{\partial\theta}{\partial y}=\frac{(1+\tau\theta)}{\Pr}\frac{\partial^2\theta}{\partial y^2}+\frac{\tau}{\Pr}\left(\frac{\partial\theta}{\partial y}\right)^2+\frac{(S-N)}{\Pr}\theta+Ec\left(\frac{\partial U}{\partial y}\right)^2+bU^2 \tag{11}$$

$$\frac{\partial C}{\partial t}-\alpha\frac{\partial C}{\partial y}=\frac{1}{Sc}\frac{\partial^2 C}{\partial y^2}+S_0\frac{\partial^2\theta}{\partial y^2}-KrC \tag{12}$$

From equation (5), initial and boundary conditions are:

$$\begin{aligned} &t\le 0\ \&\ \text{y<0}: U(y,t)=0,\ \theta(y,t)=0, C(y,t)=0\\ &t>0\ \&\ \text{y=0}: U(y,t)=0,\ \theta(y,t)=1, C(y,t)=1\\ &\qquad U(\infty,t)=0,\ \theta(\infty,t)=0, C(\infty,t)=0\end{aligned} \tag{13}$$

Where $U, \Pr, b_1, \theta, C, Sc, Ec, Gc, M, K, N, \alpha, \tau, Kr, b, Gr, S, So$ represent dimensionless velocity, Prandtl number, inertia number, dimensionless temperature, dimensionless species concentration, Schmidt number, Eckert number, mass Grashof number, magnetic field, porosity, radiation, suction, variable thermal conductivity, chemical reaction, dimensionless Joule-heating parameter, thermal Grashof number, heat source parameters and Soret number.

4. Numerical Procedure

Equations (10-12) are 2nd order non-linear coupled PDE together with both conditions from the equation (13). So, these equations (10-13) are resolved using the Crank-Nicolson implicit finite-difference scheme. Therefore, finite-difference equations are mentioned below:

$$\begin{aligned} &-r_1U_{i-1}^{j+1}+(1+2r_1)U_i^{j+1}-r_1U_{i+1}^{j+1}=r_2U_{i-1}^{j}+(-r_4-\alpha r_3-2r_2+1)U_i^j+\\ &(\alpha r_3+r_2)U_{i+1}^j+\Delta tGr\theta_i^j+Gc\Delta tC_i^j-b_1\Delta t\left(U_i^j\right)^2\end{aligned} \tag{14}$$

$$\begin{aligned} &-qr_1\theta_{i-1}^{j+1}+(\Pr+2qr_1)\theta_i^{j+1}-qr_1\theta_{i+1}^{j+1}=qr_2\theta_{i-1}^j+(\Pr-2qr_2-\alpha\Pr r_3-N\Delta t+S\Delta t)\theta_i^j+\\ &(qr_2+\alpha\Pr r_3)\theta_{i+1}^j+\tau r_5\left(\theta_{i+1}^j-\theta_{i-1}^j\right)^2+\Pr Ecr_5\left(U_{i+1}^j-U_{i-1}^j\right)^2+\Pr\Delta tb\left(U_i^j\right)^2\end{aligned} \tag{15}$$

$$\begin{aligned} &-r_1C_{i-1}^{j+1}+(Sc+2r_1)C_i^{j+1}-r_1C_{i+1}^{j+1}=r_2C_{i-1}^j+(Sc-2r_2-\alpha Scr_3-KrSc\Delta t)C_i^j+\\ &(r_2-\alpha r_3Sc)C_{i+1}^j+2ScS_0r_1\theta_{i-1}^j-4ScS_0r_1\theta_i^j+2ScS_0r_1\theta_{i+1}^j\end{aligned} \tag{16}$$

where

$$r_1=r_2=\frac{\Delta t}{2(\Delta y)^2}, r_3=\frac{\Delta t}{\Delta y}, r_4=\Delta t\left(M+\frac{1}{K}\right), r_5=\frac{\Delta t}{4(\Delta y)^2}, q=1+\tau\theta_i^j \tag{17}$$

Here (i,j) is an arbitrary grid point in the discrete mesh system. Where indices i and j refer to y and t respectively. The discrete mess system can be divided by rectangles with length $\Delta y=0.1$ and width $\Delta t=0.001$. Also, consider $i_{\max}=200$ and $j_{\max}=500$. Define $\mathrm{U}_i^j=U(i,j)$ for every grid point (i,j). Then, the equation (13) can be expressed in terms of finite-difference form for any i, j

$$\begin{aligned} &U(i,\ 0)=\ 0,\quad U(0,\ j)=\ 0,\quad U(i_{max},\ j)=\ 0\\ &\theta\ (i,\ 0)=0,\quad \theta(0,\ j)\ =\ 1,\quad \theta(i_{max},\ j)\ =\ 0\\ &C(i,\ 0)=\ 0,\quad C(0,\ j)\ =\ 1,\quad C(i_{max},\ j)\ =\ 0\end{aligned} \tag{18}$$

From the equations (14-16) with the above initial and boundary conditions, every internal node of each time step constitutes a tridiagonal matrix. The dimension of the tridiagonal matrix is $i_{\max}-1\times i_{\max}-1$ (i.e. 199 $\times$ 199). The tridiagonal matrix system of equations can be resolved by the Thomas algorithm for solving $i_{\max}-1$ (i.e. 199) equations with $i_{\max}-1$ (i.e. 199) unknown for each time step. Since it is a coupled equation, we started to compute the concentration and temperature distributions at each time step from equation (16) and equation (15), respectively, and then calculated values are used to compute the velocity distribution at each time step from equation (14) which meets the convergence criteria. The non-dimensional parameters, which are the skin friction coefficient, Nusselt and Sherwood numbers, can be calculated by the following formulas, respectively:

$$Cf=\frac{\partial U}{\partial y}, Nu=-\frac{\partial \theta}{\partial y}, Sh=-\frac{\partial C}{\partial y} \text{ at y=0} \tag{19}$$

5. Results and Discussion

Mathematical equations are formulated and solved numerically for the problem on Soret and variable thermal conductivity effects on heat and mass transfer flow past an infinite vertical plate. To report the characteristics of the fluid flow, which are velocity, temperature and species concentration distributions were presented for different non-dimensional parameters by graphs. Thermal Grashof number Gr, variable thermal conductivity τ, Schmidt number Sc, chemical reaction Kr, Eckert number Ec, Prandtl number $\Pr$, Joule-heating parameter b, magnetic field M, Soret number So, porosity K, mass Grashof number Gc, radiation N, Inertia number b_1, heat source S, suction α, and reaction order n are parameters and their corresponding variable. The values of parameters are fixed throughout the simulations except for, in any case, expressed. That is Gr =1.00, τ =0.10, Sc = 0.62, Kr =0.10, Ec =0.01, $\Pr$ = 0.71, b =1.00, M =1.00, So =1.00, K =1.00, Gc =1.00, N =0.10, b_1 =1.00, S =1.00, α = 1.00, n =1.00.

Velocity distributions are presented from Fig. 2 to Fig. 6 for diverse values of $N, \alpha, \tau, Kr,$ and So. The effect of N on U is presented in Fig. 2. It is found that augmenting values of N causes a decrease in U. Since increasing values of N corresponding to the rise in dominance of conduction over radiation give a reduction in fluid velocity. The influence of α on U completely coincides with the effect of the radiation parameter as clearly observed in Fig. 3. Fig. 4 presents the effect of τ on U. It is identified fluid velocity increases with increasing τ. Apart from that, Kr on the velocity profile is opposite to that of τ as clearly observed in Fig. 5. Fig. 6 displays the Soret effect So on U for So =2.5, 4.5, 6.5. Observe U increases as So increases. This is quite the opposite of the chemical reaction Kr.

Temperature distributions are presented from Fig. 7 to Fig. 9 for diverse values of $\alpha, \tau,$ and S. The effect of α on θ is plotted in Fig. 7. It is observed that θ decreases whenever α increased. Fig. 8 demonstrates θ rises with an increment in the values of τ, and in the same way for Fig. 9, θ increase for the growth in the values of S.

Concentration distributions are plotted from Fig. 10 to Fig. 13 for diverse values of $Sc, \alpha, Kr,$ and So. The effect of Sc on C is presented in Fig. 10. The trend shows C reduction with augmented values of Sc due to the increase of Sc means to fall in molecular diffusion. Fig. 11 sketched the effect of α on C. It is noticeable that the non-dimensional concentration falls with an increment of α. The influence of Kr on C is shown in Fig. 12. It can be observed from the figure, C decreases whenever the values of Kr increase. Because of the large values of Kr to decrease the thickness of the solutal boundary layer and raise the mass transfer of the fluid. The influence of So on C opposes the influence of chemical reaction Kr as shown in Fig. 13.

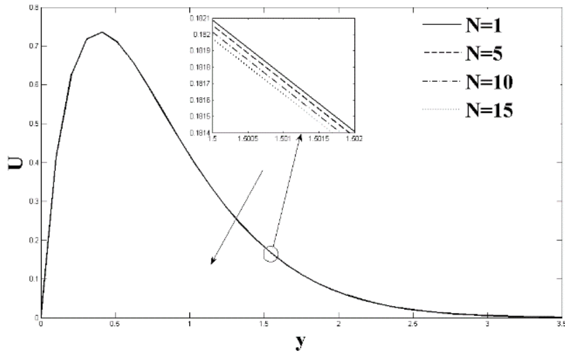

Fig. 2. Velocity against y for N =1, 5, 10, and 15.

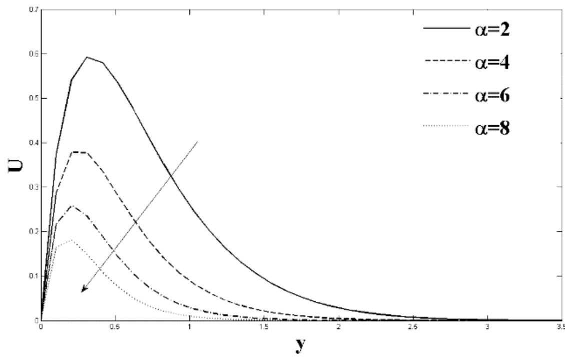

Fig. 3. Velocity against y for α =2, 4, 6 and 8.

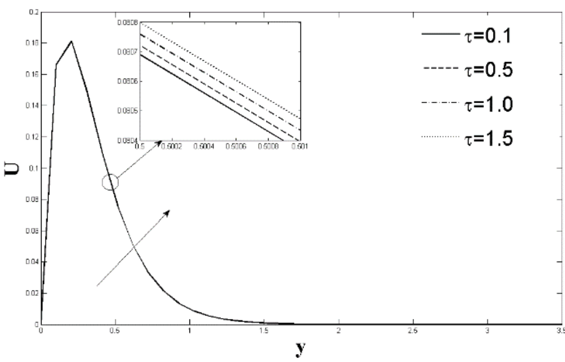

Fig. 4. Velocity against y for τ =0.1, 0.5, 1.0, and 1.5.

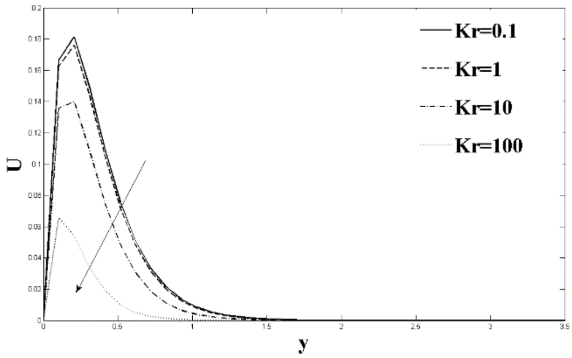

Fig. 5. Velocity against y for Kr =0.1, 1, 10, and 100.

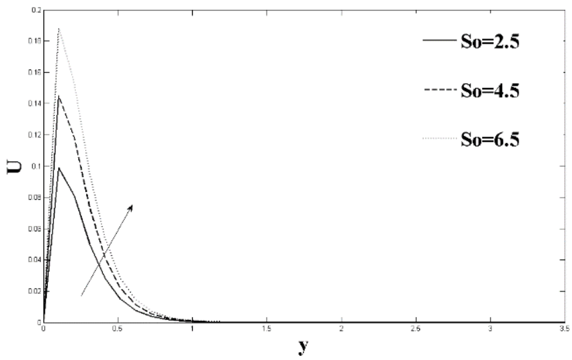

Fig. 6. Velocity against y for So = 2.5, 4.5, and 6.5.

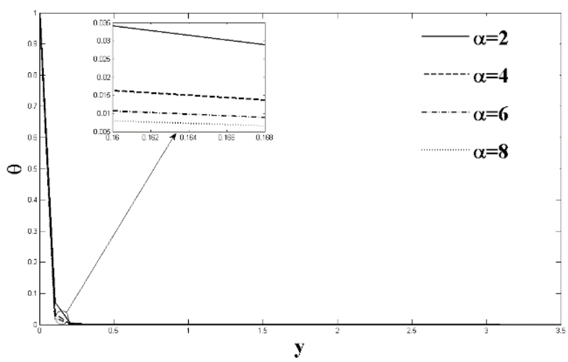

Fig. 7. Temperature against y for α =2, 4, 6, and 8.

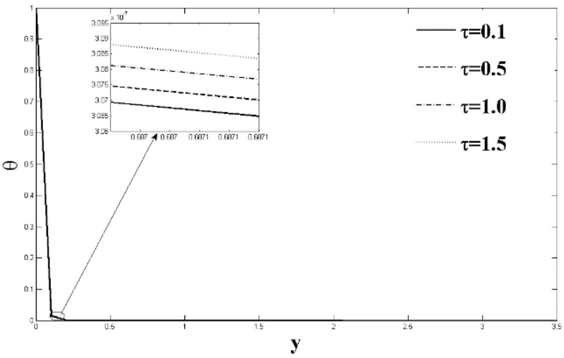

Fig. 8. Temperature against y for τ =0.1, 0.5, 1, and 1.5.

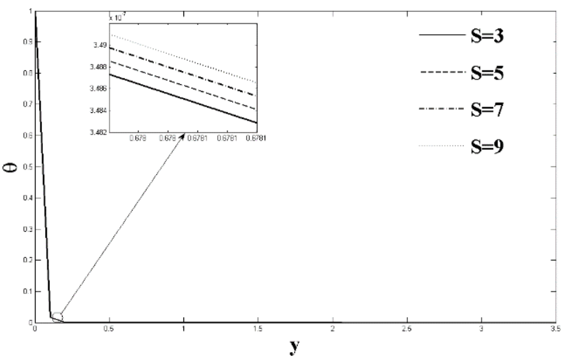

Fig. 9. Temperature against y for S =3, 5, 7, and 9.

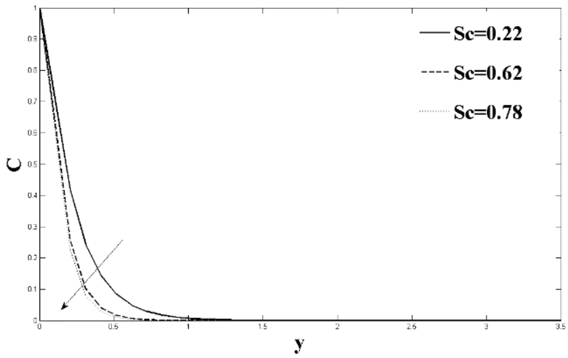

Fig. 10. Concentration against y for Sc = 0.22, 0.62, and 0.78.

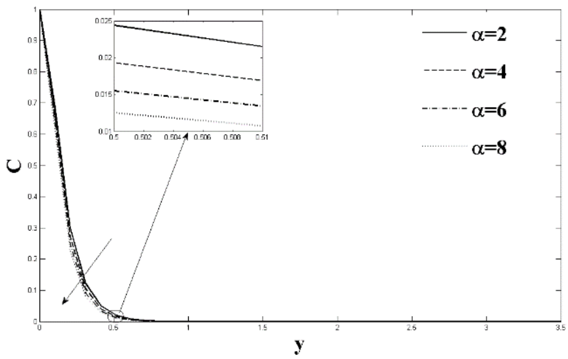

Fig. 11. Concentration against y for α = 2, 4, 6, and 8.

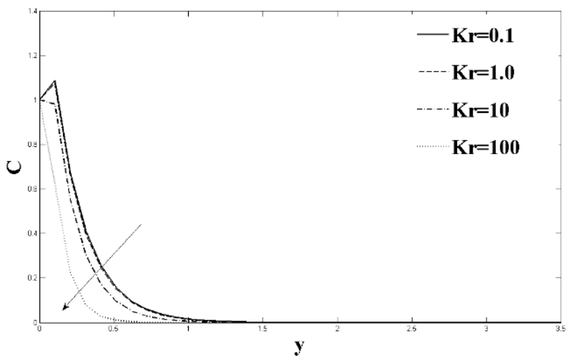

Fig. 12. Concentration against y for Kr = 0.1, 1.0, 10, and 100.

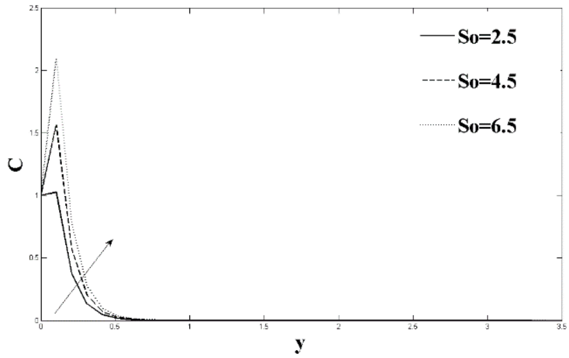

Fig. 13. Concentration against y for So = 2.5, 4.5, and 6.5.

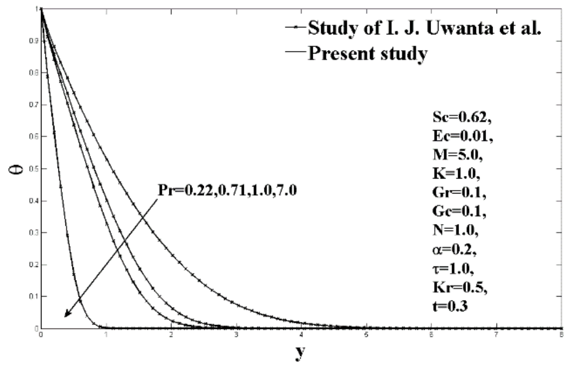

Fig. 14. Comparison of present results with that obtained by Uwanta et al. (2013) with $b_1 = 0, So = 0, S = 0, b = 0$.

Fig. 14 exhibits the validity of the outcomes compared with the fluid temperature for values of $\Pr$. We equate the outcomes with the existing outcomes obtained by Uwanta et al. (2013) by removing the inertia number, Joule-heating parameter, heat source, and Soret parameters. It shows that there is complete concurrence in their results.

Tables 1-3 present the non-dimensional values of coefficient of Skin friction (Cf) and numbers of Nusselt (Nu) and Sherwood (Sh) for the numerical solution of governing equations. Table 1 displays the influence of non-dimensional parameters $\Pr, \alpha, Gr, So, Sc, Kr, M, N, S$ and Gc on Cf . In table 1, it is observed that the augmenting values of Pr, Kr, M, N, Sc and α lead to a decline in Cf , but for ascending values of Gr, Gc, S and So rises in Cf . Table 2 presents the influence of non-dimensional parameters $\Pr, Gr, N, b, \alpha$ and So on Nu . From Table 2, it can be observed that Nu rises with the increase of values of $\Pr, N$ and α but the increase in values of Gr, b and So results in fall of Nu . Similarly, table 3 exhibits the influence of non-dimensional parameters Sc, Kr, α and So on Sh . Results from table 3 show that Sh increases whenever the values of Sc, Kr and α increase, but increasing So leads to a decrease of Sh .

6. Conclusions

Soret and variable thermal conductivity effect on the unsteady hydro-magnetic free convective with heat and mass transfer flow past an infinite vertical plate through a porous medium have been studied thoroughly. The influence of chemical reaction, Joule-heating parameter, suction, and radiation are considered on it. This problem has been investigated numerically using the implicit finite-difference scheme. The results were discussed through graphs and tables for non-dimensional parameters. The significant conclusions are made as follows.

- The influence of N, α, Kr and So on Cf is coincidental with the velocity U of the fluid.
- The influence of α and So on Nu is quite the opposite to that of the temperature θ of the fluid.
- The influence of Sc, α, Kr and So on Sh is quite the opposite to that of the concentration C of the fluid.
- The effect of concentration C of the fluid rises with an increased Soret number So whereas reduces in Sherwood number Sh .
- N, α and Kr tend to decrease the velocity U whereas they rise with augmenting values of τ and So.
- The fluid temperature θ rises with increasing values of τ and S whereas it reduces with an increment of α .
- Soret number So tends to increase the concentration C whereas it declines with augmenting the values of Kr, α and Sc.

Pr	Gr	Gc	Sc	Kr	α	M	N	S	So	Cf
0.71	1	1	0.62	0.1	1	1	0.1	1	1	0.7145
1										0.6811
	5									2.0936
	8									3.1401
		5								2.1216
		8								3.1231
			0.78							0.6967
			0.90							0.6857
				1						0.6871
				2						0.6617
					4					0.5248
					6					0.3742
						5				0.5340
						10				0.4143
							1			0.6898
							5			0.6305
								3		0.8042
								5		0.9927
									2.5	0.7927
									4.5	0.8957

Table 1. Coefficient of Skin friction.

Pr	Gr	N	b	α	So	Nu
0.71	1	0.1	1	1	1	0.5522
1						0.8803
	5					0.4924
	8					0.4092
		1				0.9379
		5				1.9686
			10			0.4766
			50			0.1155
				4		1.8389
				6		2.6383
					2.5	0.5484
					4.5	0.5422

Table 2. Nusselt number.

Sc	Kr	α	So	Sh
0.62	0.1	1	1	0.7722
0.78				0.8853
	1			1.0320
	2			1.2747
		4		1.1867
		6		1.5564
			2.5	0.4890
			4.5	0.1187

Table 3. Sherwood number.

References

Abel MS, Siddheshwar PG, Mahesha N (2009). Effects of thermal buoyancy and variable thermal conductivity on the MHD flow and heat transfer in a power-law fluid past a vertical stretching sheet in the presence of a non-uniform heat source, Int. J. Non. Linear. Mech., 44(1), 1-12.

Ahmed N, Sengupta S, Datta D (2013). An Exact Analysis for Mhd Free Convection Mass Transfer Flow Past an Oscillating Plate Embedded in a Porous Medium With Soret Effect, Chem. Eng. Commun., 200(4), 494-513.

Ahmed S, Kalita K (2013). Analytical and Numerical Study for MHD Radiating Flow over an Infinite Vertical Surface Bounded by a Porous Medium in Presence of Chemical Reaction, Jou. of Applied Fluid Mechanics, 6(4), 597-607.

Chamkha AJ (2004). Unsteady MHD convective heat and mass transfer past a semi-infinite vertical permeable moving plate with heat absorption, Int. J. Eng. Sci., 42, 217-230.

Idowu AS, Falodun BO (2019). Soret–Dufour effects on MHD heat and mass transfer of Walter's-B viscoelastic fluid over a semi-infinite vertical plate: spectral relaxation analysis, J. Taibah Univ. Sci., 13(1),49-62.

Javaherdeh K, Mirzaei NN, Moslemi M (2015). Natural convection heat and mass transfer in MHD fluid flow past a moving vertical plate with variable surface temperature and concentration in a porous medium, Eng. Sci. Technol. an Int. J., 18(3),423-431.

Jha BK (1994). MHD flow through porous medium in presence of heat and mass transfer with heat source, Polym. Plast. Technol. Eng, 33(6), 793-801.

Krishna MV, Reddy MG (2018). MHD Free Convective Boundary Layer Flow through Porous medium Past a Moving Vertical Plate with Heat Source and Chemical Reaction, Mater. Today Proc., 5, 91-98.

Krishna MV, Swarnalathamma BV, Chamkha AJ (2019). Investigations of Soret, Joule and Hall effects on MHD rotating mixed convective flow past an infinite vertical porous plate, J. Ocean Eng. Sci., 4, 263-275.

Mohamadien GF (2012). The effect of thermal dispersion on unsteady MHD convective heat transfer through vertical porous, NRIAG J. Astron. Geophys.,1(2), 114-118.

Murthy SVSSNVGK, Kumar V (2018). MHD forces on double diffusive free convection process along a vertical wavy surface embedded in a doubly stratified fluid-saturated Darcy porous medium under the influence of Soret and Dufour effect, Eur. J. Comput. Mech., 27(1), 33-57.

Praveena D, Varma SVK, Veeresh C, Raju MC (2017). Chemical reaction and heat source effect on MHD free convection flow of a micropolar fluid through a porous medium over a semi-infinite moving plate with constant heat and mass flux, J. Inf. Optim. Sci., 38(8), 206-212.

Reddy PC, Raju MC, Raju GSS (2016). Magneto-hydrodynamic convective double diffusive laminar boundary layer flow past an accelerated vertical plate, Int. J. Eng. Res. Africa, 20,80-92.

Reddy PC, Raju MC, Raju GSS (2018). MHD Natural convective heat generation/absorbing and radiating fluid past a vertical plate embedded in porous medium - an exact solution, J. Serbian Soc. Comput. Mech., 12(2), 106-127.

Reddy KS, Reddy PC, Raju GSS (2018). Thermal Diffusion and Joule Heating Effects on MHD Radiating Fluid Embedded in Porous Medium, Int. J. Res. Eng. Appl. Manag., 04(04), 2454-9150.

Sarma D, Pandit KK (2016). Effects of Hall current, rotation and Soret effects on MHD free convection heat and mass transfer flow past an accelerated vertical plate through a porous medium, Ain Shams Eng. J., 1-16.

Sharma PK (2005). Influence of periodic temperature and concentration on unsteady free convective viscous incompressible flow and heat transfer past a vertical plate in slip-flow regime, Matemáticas Enseñanza Univ., 13(1), 51-62.

Uwanta IJ, Sani M (2013). Heat and Mass Transfer Flow Past an Infinite Vertical Plate with Variable Thermal Conductivity, Int. J. Appl. Inf. Syst., 6(1), 16-24.

Uwanta IJ Sani M (2014). Heat Mass Transfer Flow past an Infinite Vertical Plate with Variable Thermal Conductivity, Heat Source and Chemical Reaction, Int. J. Eng. Sci., 3(5), 77-89.